Geochemistry, Geophysics, Geosystems

Supporting Information for

Magnetic mineral populations in lower oceanic crustal gabbros (Atlantis Bank, SW Indian Ridge): Implications for marine magnetic anomalies

J.A. Bowles[1], A. Morris[2], M.A. Tivey[3], and I. Lascu[4]

[1] Department of Geosciences, University of Wisconsin - Milwaukee, Milwaukee, WI, USA
[2] School of Geography, Earth and Environmental Sciences, University of Plymouth, Plymouth, UK
[3] Department of Geology and Geophysics, Woods Hole Oceanographic Institution, Woods Hole, MA, USA
[4] Department of Mineral Sciences, National Museum of Natural History, Smithsonian Institution, Washington, DC, USA

Contents of this file

Additional Supporting Information (Files uploaded separately)

Table S1 (Excel file)

Introduction

This supplementary file contains supporting figures S1 and S2 which provide example NRM demagnetization data showing evidence of gyroremanent magnetization (GRM) acquisition; supporting figures S3 and S4 with additional details regarding the first order reversal curve (FORC) principal component analysis; supporting figure S5 which shows FORC endmember variation as a function of saturation magnetization; and supporting figure S6 with details on remanence recovery after cycling from room temperature to 10K and back to room temperature. Table S1 provides a summary of rock magnetic properties for all samples.

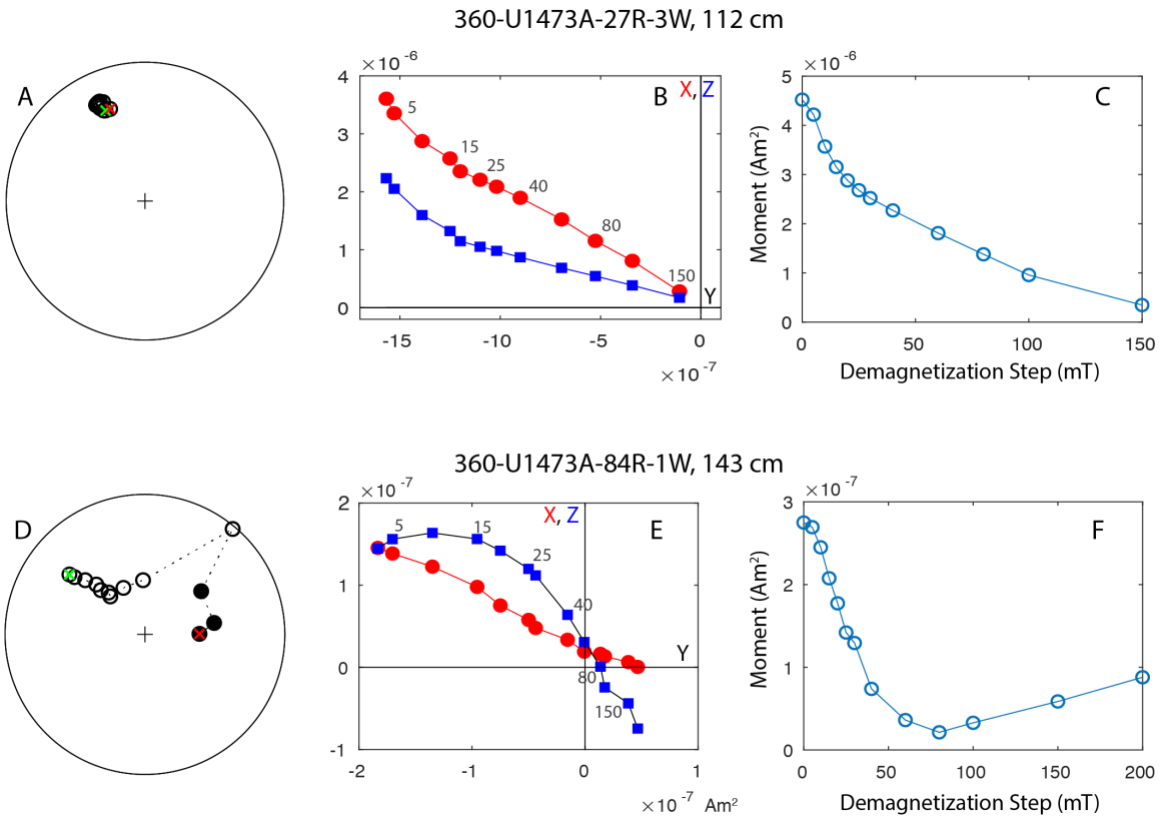

Figure S1. Example alternating field demagnetization data of unoriented samples. Top panels show well-behaved sample with a stable direction during demagnetization and a moment that monotonically decays to near zero. Bottom panels show poorly-behaved data that do not result in a stable direction and a moment that decreases and then increases again. This behavior appears to be associated with acquisition of a gyroremanent magnetization (See Fig. S2). The behavior is *not* consistent with acquisition of a spurious ARM; because the direction of the applied AF field alternated between +X/+Y/+Z and -X/-Y/-Z, an ARM acquisition should produce a zig-zag behavior in the directions that is not observed. (A,D) Equal-area projection. Closed symbols lower hemisphere; open symbols upper hemisphere. Green 'X' superimposed on first measurement; red 'X' superimposed on last measurement. (B,E) Vector endpoint diagrams in magnetometer coordinates. Red circles are Y-X projections; blue squares are Y-Z projections. (C,F) Total moment during demagnetization.

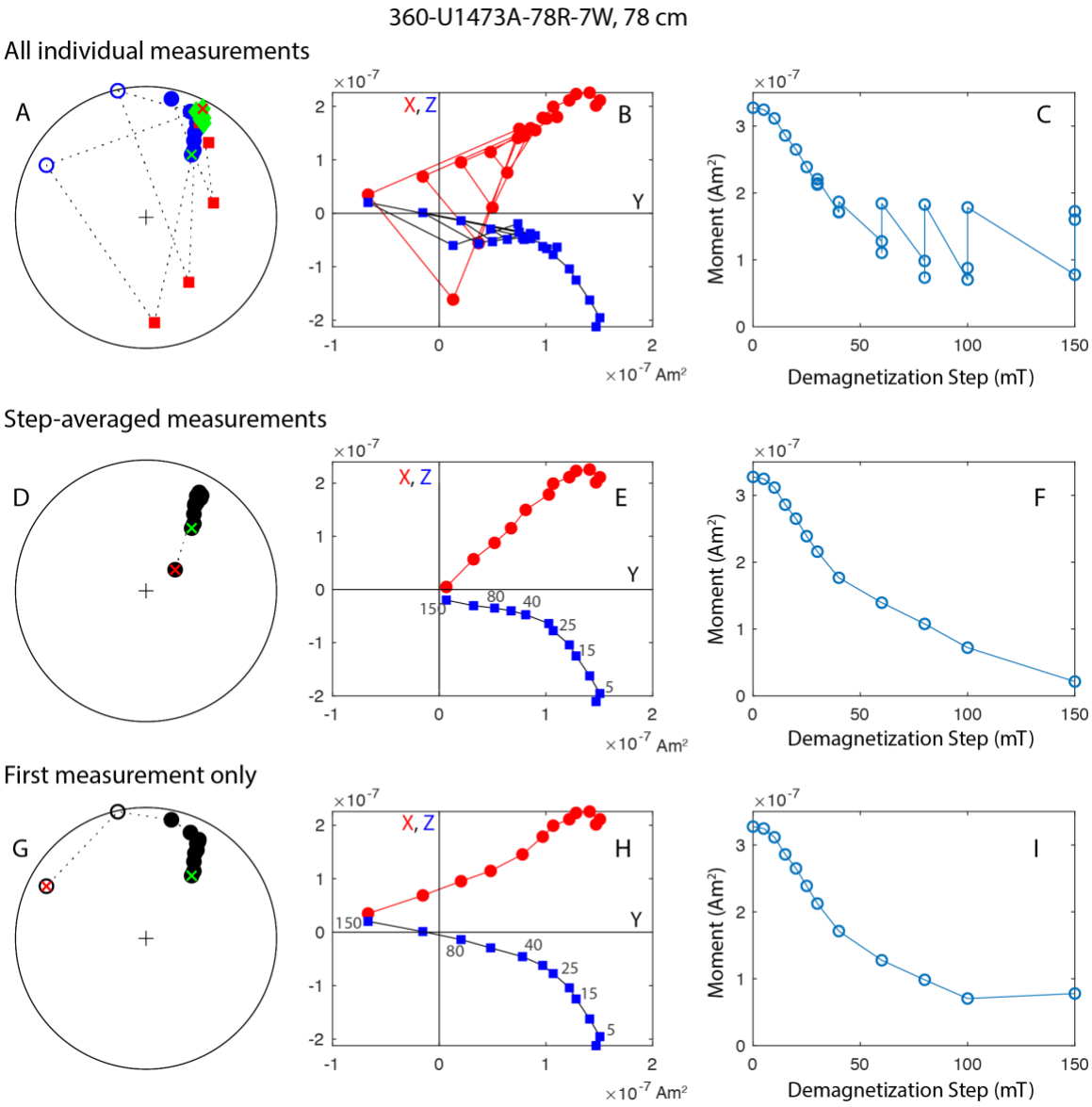

Figure S2. Example data from sample 360-U1473A-78R-7W, 78 cm that underwent the triple-demagnetization alternating field (AF) scheme to average out acquisition of a gyroremanent magnetization (GRM). See main text for details. Top panels show all individual measurements, including the three measurements for each step ≥30 mT. With increasing applied alternating field, the directional deviation increases. Middle panels show step-averaged measurements, which largely eliminate the large directional swings. Bottom panels show data from only the first measurement at each step. This is analogous to the standard treatment most samples received (single-demagnetization only). (A,D,G) Equal-area projection. Closed symbols lower hemisphere; open symbols upper hemisphere. Green 'X' superimposed on first measurement; red 'X' superimposed on last measurement. In panel A, symbols indicate demagnetization protocol immediately prior to measurement. For ≥30 mT, treatment was in the following order: demagnetization along X-Y-Z (blue circles); demagnetization along Y (red squares); demagnetization along X (green diamonds). (B,E,H) Vector endpoint diagrams in magnetometer coordinates. Red circles are Y-X projections; blue squares are Y-Z projections. (C,F,I) Total moment during demagnetization.

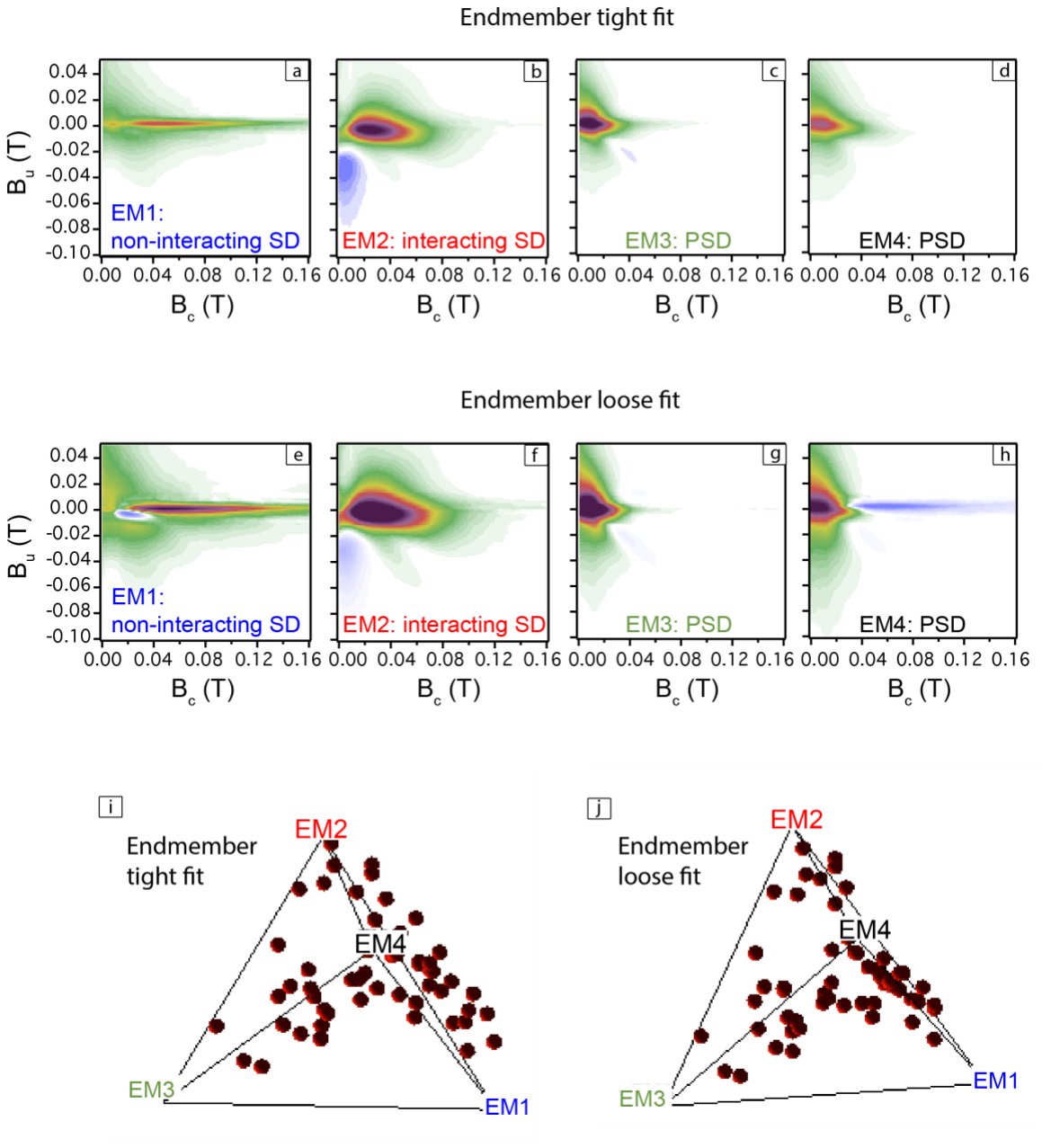

Figure S3. Endmembers chosen for FORC principal component analysis (Lascu et al., 2015; Harrison et al., 2018). (a-d) Tight fit to data results in more physically realistic endmembers, but a significant number of points that fall outside the mixing tetrahedron (i). (e-h) A looser fit to the data results in a higher percentage of data points falling inside the tetrahedron (j), but less physically-realistic endmembers. (i-j) Quaternary diagrams showing the relative abundance of each component for all the samples. See also Fig. 1d in the main text.

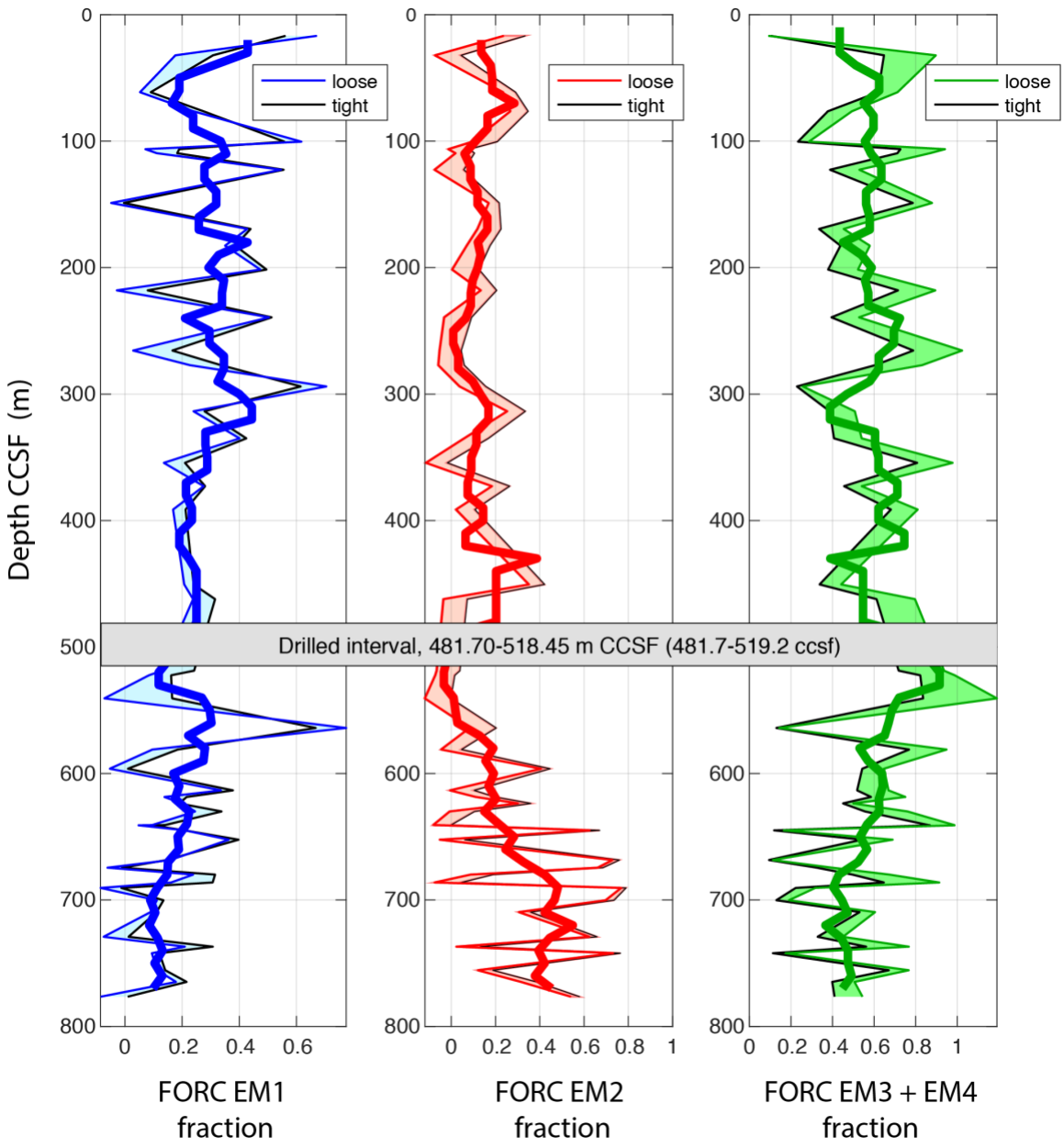

Figure S4. Downhole variation in FORC endmember abundance for loose fit (colored lines) and tight fit (black lines). An average of these two fits was used in the final analysis, but the difference approximates the uncertainty in the fits. See main text and Figure S3. A 60-m running average is shown by the thick lines.

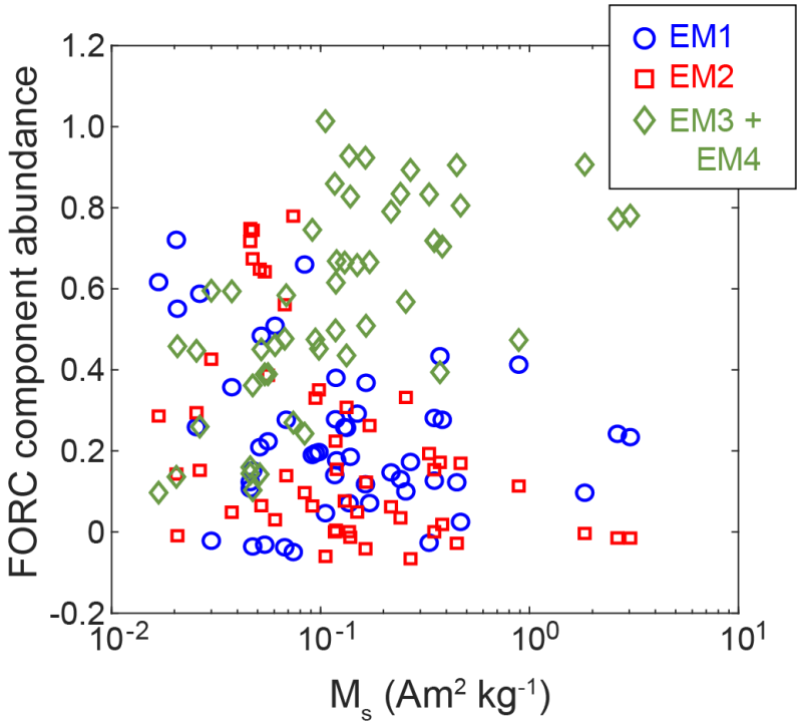

Figure S5. Variation in FORC endmember abundance with saturation magnetization (M_s). The dominance of the two 'PSD' endmembers (EM3 and EM4) with increasing M_s suggests that these endmembers are associated with the coarse magmatic oxides.

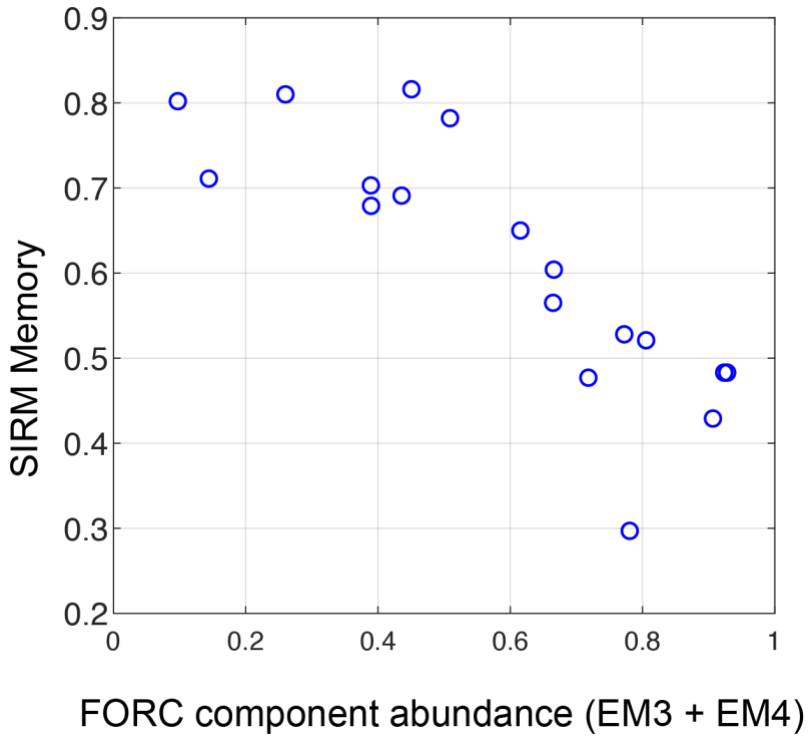

Figure S6. SIRM memory as a function of the abundance of 'PSD' FORC endmembers (EM3 + EM4). SIRM memory is the remanence remaining after cycling the SIRM300K remanence to 10 K and back to 300 K, through the Verwey transition. A reduction in memory is associated with irreversible spin rotations and/or wall motions associated with 'PSD' or MD magnetite.

Table S1. Magnetic Properties. Table uploaded as separate Excel document. Data columns:

1. Sample ID: in the form of Expedition (360) - Hole (U1473A) - Core - Section, depth in section (cm)
2. Lithology (as described by shipboard scientists in MacLeod et al., 2017a)
3. Depth: meters core composition depth below seafloor (CCSF)
4. NRM: volume normalized natural remanent magnetization (A/m)
5. NRM: mass normalized natural remanent magnetization (Am^2/kg)
6. MDF: median destructive field (mT)
7. M_s: saturation magnetization (Am^2/kg)
8. M_{rs}: saturation remanent magnetization (Am^2/kg)
9. M_{rs}/M_s: remanence ratio of saturation remanent magnetization / saturation magnetization
10. B_c: coercivity (mT)
11. B_{cr}: coercivity of remanence (mT)
12. EM1: end-member 1 from FORC PCA analysis (non-interacting single domain)
13. EM2: end-member 2 from FORC PCA analysis (interacting single domain)
14. EM3: end-member 3 from FORC PCA analysis (pseudo-single domain)
15. EM4: end-member 4 from FORC PCA analysis (pseudo-single domain)
16. LT data: * indicates that low-temperature remanence data were collected for this sample
17. Il_{50}: * indicates sample lost a significant fraction of a 10K IRM on warming to 50K (consistent with ilmenite)
18. T_v: Verwey transition temperature (K)
19. T_{c1}: Dominant (higher) Curie temperature (°C)
20. T_{c2}: Secondary (lower) Curie temperature (°C)
21. X(T) hump: * indicates a presence of a hump in the thermomagnetic warming curve, indicating hydrothermal alteration
22. ΔX_{100}: percent change in susceptibility at 100°C between warming and cooling curves